Available online at www.sciencedirect.com
ScienceDirect
Journal of Molecular Catalysis A: Chemical 263 (2007) 103–111
JOURNAL OF MOLECULAR CATALYSIS A: CHEMICAL
www.elsevier.com/locate/molcata

Structure of $MgCl_2$–$TiCl_4$ complex in co-milled Ziegler–Natta catalyst precursors with different $TiCl_4$ content: Experimental and theoretical vibrational spectra

Luigi Brambilla [a], Giuseppe Zerbi [a,*], Fabrizio Piemontesi [b], Stefano Nascetti [b], Giampiero Morini [b]

[a] *Dipartimento di Chimica, Materiali e Ingegneria Chimica "Gulio Natta", NanoEngineered MAterials and Surfaces (NEMAS), Center of Excellence for Nanostructured Materials and Surfaces Engineering Politecnico di Milano, Piazza Leonardo Da Vinci 32, 20133 Milano, Italy*

[b] *Basell Polyolefins, Centro Ricerche G. Natta, 44100 Ferrara, Italy*

Received 5 June 2006; received in revised form 28 July 2006; accepted 1 August 2006
Available online 25 September 2006

Abstract

The FT-Raman spectra of a series of mechanically prepared $MgCl_2$–$TiCl_4$ samples with increasing content of $TiCl_4$ have been recorded. Raman scattering lines in the range 600–100 cm^{-1} reveal the formation of $TiCl_4$ molecules complexed on the lateral cuts of activated $MgCl_2$ crystals. This pattern of lines suggests that atleast three types of complexes are formed during the grinding process and their relative concentration depend on the starting concentration of $TiCl_4$. Two types of these complexes have been shown to be unstable and easily removed when the samples are washed with *n*-hexane. In the former two cases $TiCl_4$ molecules are seemingly physisorbed and/or weakly complexed on $MgCl_2$. The remaining complex is stable and it is found in every sample also after washing. This stable complex shows Raman lines which can be interpreted as originated from the complexed $TiCl_4$ molecules with the Ti atoms in an octahedral coordination. On the other hands also monomeric $TiCl_4$ species complexed along the (1 1 0) lateral cut or dimeric $TiCl_4$ species complexed along the (1 0 0) lateral cuts of the $MgCl_2$ crystal can take up a geometry with the Ti in an octahedral coordination. Both these structures have been considered in this work. Calculated Raman spectra, molecular energy considerations and Raman lines intensity ratios strongly support the fact that the stable complexes are the monomeric $TiCl_4$ species complexed along the (1 1 0) $MgCl_2$ lateral cuts. A spectroscopic quantitative determination of the complexed $TiCl_4$ for this class of material is proposed.

Keywords: Ziegler–Natta catalysts; $TiCl_4$–$MgCl_2$ complex; FT-Raman spectroscopy; DFT quantum chemical calculation

1. Introduction

Modern Ziegler–Natta catalysts for the industrial production of polyolefins are based on $TiCl_4$ supported on activated $MgCl_2$ [1]. The role of $MgCl_2$ is not only the dispersion of the titanium atoms over a high surface area, thus increasing the number of active sites, but it is also able to activate the polymerization reaction by increasing the propagation constant with respect to the older $TiCl_3$-based systems. The bonding of $TiCl_4$ molecules on $MgCl_2$ surface and the structure of the generated sites active in polymerization are still not completely clear. Starting from experimental evidence, the formation of preferential cuts on $MgCl_2$ crystallites corresponding to (1 0 0) and (1 1 0) planes was suggested [2]. On these coordinatively unsaturated Mg^{2+} ions the chemisorption of $TiCl_4$ molecules is likely to occur and a variety of active site structures have been proposed [3,4]. However, the experimental validation of some of these catalytic complex structures is still missing. In fact, most of the infrared studies [5–11] have been devoted to define the complexes between the catalyst precursors and the electron donors added in order to improve the stereospecificity in 1-olefin polymerization. Recently, the specific interactions between $TiCl_4$ and metallic Mg films grown on Au surface have been studied by means of X-ray photoelectron

* Corresponding author. Tel.: +39 02 23993235; fax: +39 02 23993231.
E-mail address: giuseppe.zerbi@polimi.it (G. Zerbi).

1381-1169/$ – see front matter © 2006 Elsevier B.V. All rights reserved.
doi:10.1016/j.molcata.2006.08.001

spectroscopy (XPS) [12] and reflection absorption infrared spectroscopy (RAIRS) [13].

In our previous paper [14] the application of Raman spectroscopy to the study of $TiCl_4$ complexes on a co-milled $MgCl_2/TiCl_4$ catalyst precursor was presented. The interpretation of the spectrum was carried out with the help of vibrational spectroscopic correlations and quantum chemical calculations. These preliminary results indicated the formation of an octahedral $TiCl_4$ species on the (1 1 0) lateral cut of $MgCl_2$.

The aim of this study is to find further support to our previous result by focussing our attention on a series of catalyst precursors with different content of $TiCl_4$ (Mg/Ti molar ratio in the range from 15.7 to 46 mol/mol). The effect of different preparation method on the $MgCl_2/TiCl_4$ complexes is also considered.

Raman spectroscopy turns out to be a very powerful technique to study this system, giving detailed and selective information at molecular level that have been interpreted with the help of high level quantum chemical calculations.

2. Experimental

All samples have been prepared and handled in an inert atmosphere. Pure $MgCl_2$ and $TiCl_4$ were purchased from Aldrich and used without further purification.

2.1. Co-milled $MgCl_2/TiCl_4$

Under inert atmosphere about 10 g of $MgCl_2$ and the amount of $TiCl_4$ needed to reach the desired Mg/Ti ratio (see Table 1) were charged in a ball mill. The milling of the mixture was carried out for 4 h and then discharged. Part of every samples was washed with hexane and carefully dried under vacuum. Elemental analyses to determine Ti and Mg contents were carried out only on the washed samples.

2.2. Samples from chemically activated $MgCl_2$

In a flask 350 mL of dibutyl magnesium (1 M solution in *n*-heptane) and 350 mL of chlorobenzene were charged under inert atmosphere. The solution was cooled to 5 °C and gaseous HCl (obtained by slowly dropping an aqueous solution of HCl, 36% (w/v), to concentrate H_2SO_4) was continuously fed over 5 h. The temperature remained between 5 and 10 °C all the time. The HCl feeding was then stopped and the suspension warmed up to room temperature. After 1 h, the solid was recovered by filtration, washed with hexane and dried under vacuum.

In a flask, 12 g of the obtained $MgCl_2$ was suspended in 170 mL of hexane. The desired amount of $TiCl_4$ (see Table 1) was added and the temperature raised to 70 °C. After 1 h the solid was recovered and a portion of the solid was washed four times with hexane and carefully dried.

2.3. Sample from $MgCl_2 \cdot xEtOH$

In a flask 5 g of a $MgCl_2$/EtOH complex (EtOH = 25 wt.%) was added to 125 mL of $TiCl_4$ at 0 °C. The temperature was raised to 120 °C and the solid was stirred for 1 h. At the same temperature, two more treatments with fresh $TiCl_4$ were carried out. The solid was recovered, washed four times with hexane at 60 °C, one time at room temperature and finally dried under vacuum.

2.4. Analysis of the solid catalyst precursors

Titanium and magnesium were determined via inductively coupled plasma (ICP) spectrometry.

X-ray diffraction (XRD) spectra were recorded to determine the crystallite width and thickness from the intensity of the D110 reflection and of the D003 reflection, respectively [1].

The samples for the Raman analysis were prepared in a controlled atmosphere and sealed in NMR tubes suitable for Raman spectroscopy. FT-Raman spectra were recorded with a Nicolet FT-Raman module (512 scans, 4 cm^{-1} resolution and 240 mW of laser power and intensity corrected with white light internal correction). Raman spectra were recorded with a Dilor XY spectrometer using a 514.5 nm exciting line of an Ar^+ laser. The laser power at the sample was kept at few mw in order to avoid sample degradation. No spectral changes or samples burns induced by the laser were observed during the acquisitions of the spectra.

Quantum chemical calculations on molecular models were also carried out: programs and level of theory used will be specified in the text.

Table 1
Preparation and characterization of $MgCl_2/TiCl_4$ samples analyzed with Raman spectroscopy

Samples	Preparation method	Mg/Ti[a] (mol/mol)	Mg[b] (wt.%)	Ti[b] (wt.%)	Cl[b] (wt.%)	Mg/Ti (mol/mol)	X-ray diffraction	
							D110	D003
$C_{50/1}$	(1)	50	23.4	1	73.3	46.0	114	99
$C_{30/1}$	(1)	30	23.7	1.6	73.6	29.1	83	53
$C_{20/1}$	(1)	20	21.9	2.2	72.4	19.6	90	47
$C_{10/1}$	(1)	10	21.5	2.7	71	15.7	54	68
C_{chem1}	(2)	2	21.4	3.1	70.3	13.6	50	12
C_{chem2}	(2)	200	23.7	0.2	72.1	233.1	nd	nd
C_{deal}	(3)		19.8	4.5	71.8	8.6	nd	nd

Experimental conditions: (1) $MgCl_2$ and $TiCl_4$ co-milled 4 h in a ball mill; (2) activated $MgCl_2$ (obtained from Mg dialkyl and HCl) treated with $TiCl_4$ at 70 °C in hexane; (3) $MgCl_2$/ethanol complex + neat $TiCl_4$ at 120 °C.

[a] Mg/Ti molar ratio charged in the ball mill or in the reactor.

[b] Chemical analysis on samples washed with hexane (residual solvent <1.5 wt.%).

To summarize (see Table 1), the samples considered in this work are:

- samples with nominal Mg–Ti ratio of 50/1, 30/1, 20/1 and 10/1 (hereafter referred in the text as $C_{50/1}$, $C_{30/1}$, $C_{20/1}$ and $C_{10/1}$);
- the same samples washed with *n*-hexane;
- samples C_{chem1} and C_{chem2} prepared via chemical reaction starting from alkyl Mg;
- sample C_{deal} obtained from an $MgCl_2$/EtOH complex.

3. Spectroscopic results

3.1. FT-Raman and visible Raman spectra of co-milled precursors

The Raman spectra of the $MgCl_2$–$TiCl_4$ samples before and after washing with *n*-hexane are shown in Fig. 1. In every spectrum the characteristic Raman lines at 240 and 152 cm^{-1} of crystalline $MgCl_2$ [14–16] can be easily seen. Their occurrence confirms the crystalline nature of the $MgCl_2$ support in every sample independently from the $TiCl_4$ content.

In these spectra other lines which cannot be assigned to $MgCl_2$ are clearly observed near 450, 386, 290, 170 and 120 cm^{-1}. Necessarily, the origin of these lines has to be ascribed to the occurrence of $TiCl_4$ molecules somehow complexed or physisorbed on the $MgCl_2$ crystal (no other chemical species have been introduced). Comparing the spectra of unwashed samples in Fig. 1 it is possible to notice the evolution in number and intensities of these lines when the relative amount of $TiCl_4$ increases.

Starting from the Raman spectrum of the sample with the lowest Ti content ($C_{50/1}$) only the lines near 450 cm^{-1}, forming a broad and structured peak, are easily seen. Moreover, it is also possible to guess the occurrence of other lines at 290 and 170 cm^{-1} in spite of their weak intensity. In the spectrum of the $C_{30/1}$ the lines at 450, 290 and 170 cm^{-1} become stronger with a more detailed shape. In the spectrum of $C_{20/1}$ two new lines at 386 and 120 cm^{-1} are observed in addition to those at 450, 290 and 170 cm^{-1}. In the spectrum of $C_{10/1}$, all the lines at 450, 386, 290, 170 and 120 cm^{-1} are present with appreciable intensities.

On the contrary the FT-Raman spectra of the washed samples show the same spectral pattern independently from the Ti content and only the lines near 450, 290 and 170 cm^{-1} of the complexed $TiCl_4$ [14] can be observed. Necessarily, the washing procedure should have removed those $TiCl_4$ molecules which are either physisorbed or weakly complexed with $MgCl_2$ lateral cuts.

A direct comparison of the spectra of washed and unwashed samples in Fig. 1 shows that with no doubt, the lines at 386 and 120 cm^{-1} are removed by the treatment with the solvent. These lines can be safely assigned to $TiCl_4$ molecules that are physisorbed or weakly bound to the $MgCl_2$ crystal keeping the tetrahedral structure [14].

Moreover, all the washed samples show slightly lower intensities of the complex lines near 450 cm^{-1} with respect to the 240 cm^{-1} $MgCl_2$ line taken as internal reference. This can be better seen when the Raman spectra with laser exciting line at 514.5 nm of washed and unwashed $C_{20/1}$ and $C_{10/1}$ are considered (Fig. 2). In these spectra, it is possible to identify three lines that contribute to the intensity of the 450 cm^{-1} broad peak, localized at 471, 458 and 448 cm^{-1}. The washing of the samples shows a small decrease of the intensity of the 450 cm^{-1} line and, in particular, the component at 458 cm^{-1} is reduced more than the component at 448 cm^{-1}.

The dependency on washing of the lines near 450 cm^{-1} suggests that atleast two different types of complexes are present: one stable which survives the washing and one less stable (or unstable) which is removed by the solvent.

It becomes apparent that the lines located near 450 cm^{-1} (and particularly the components that survive the hexane treatment) and 290 cm^{-1} (not affected by the solvent) are the main spectroscopic markers of the stable $TiCl_4$ complex whose identification requires a careful spectroscopic analysis.

In Fig. 3, the Raman spectra with exciting line at 514.5 nm of pure $TiCl_4$ and $C_{20/1}$ are shown. As reported earlier [14], the strongest lines near 450 cm^{-1} of the stable complex derive from the triply degenerate F_2 mode originally at 511 cm^{-1} in the spectrum of pure $TiCl_4$ (tetrahedral symmetry, T_d point group).

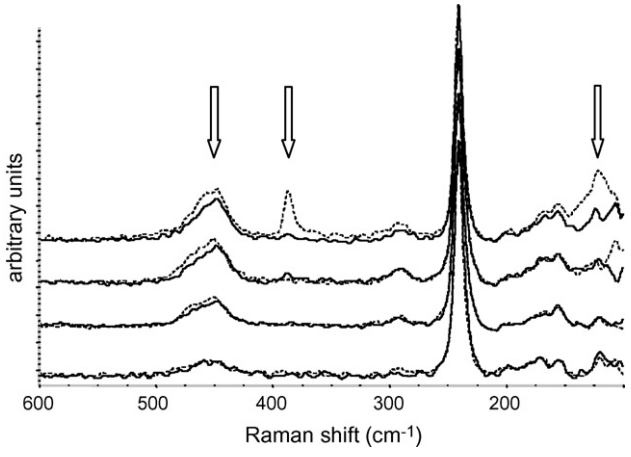

Fig. 1. Comparison between the FT-Raman spectra of washed (solid line) and unwashed (dotted line) samples: $C_{10/1}$, $C_{20/1}$, $C_{30/1}$ and $C_{50/1}$ from top. The Raman lines that change after washing are indicated by arrows.

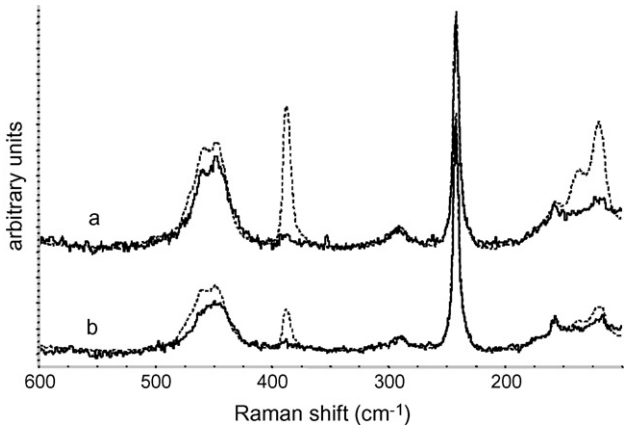

Fig. 2. Comparison between the Raman spectra with exciting line at 514.5 nm of washed (solid line) and unwashed (dotted line) $C_{10/1}$ (a) and $C_{20/1}$ (b).

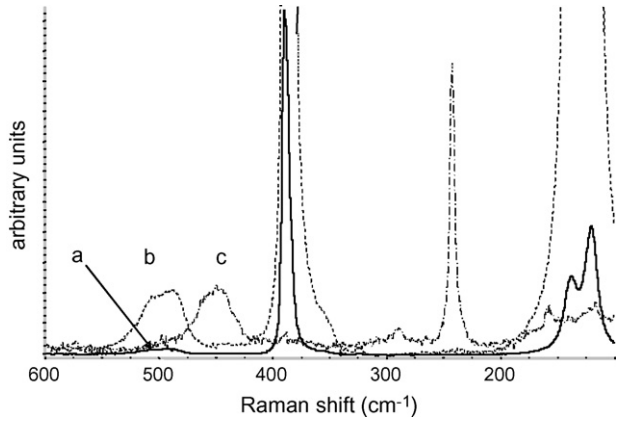

Fig. 3. Comparison between the Raman spectra with exciting line at 514.5 nm of pure $TiCl_4$ (a), pure $TiCl_4$ expanded in intensity (b) and washed $C_{20/1}$ (c).

This band is shifted in frequency and enhanced in intensity by the interaction with $MgCl_2$. This behaviour has been satisfactorily explained by quantum chemical calculations [14] as due to a change in the geometry of $TiCl_4$ from T_d to C_{2v} when it complexes with $MgCl_2$.

Some further spectroscopic considerations can be used to explain more in detail the scattering lines near 511 cm^{-1} for pure $TiCl_4$ and near 450 cm^{-1} for the $TiCl_4$ complexed on $MgCl_2$. As in the case of neat CCl_4 also for neat $TiCl_4$ [17] the triply degenerate Ti–Cl stretching $\upsilon_4(F_2)$ at 511 cm^{-1}, happens to be accompanied at close frequencies by a binary combination of modes $\upsilon_1(A_1)$ at 386 cm^{-1} and $\upsilon_3(F_2)$ at 140 cm^{-1} (346 cm^{-1} + 140 cm^{-1} = 526 cm^{-1}), thus generating a doublet which is indeed observed near 510 cm^{-1} in the experimental spectrum (spectra a and b in Fig. 3). For the isolated molecule the combination level occurs near the fundamental of F_2 species and the symmetry conditions $A_1 \otimes F_2 = F_2$ allow the existence of Fermi resonances with the fundamental of F_2 species.

On the other hand, upon complexation the frequency of $\upsilon_1(A_1)$ lowers and also the symmetry of the system lowers from T_d to C_{2v} and each of the F_2 levels υ_3 and υ_4 splits into a triplet of A_1, B_1 and B_2 species [18]. A more detailed description of this phenomenon is reported in a previous paper [14].

The vibrational analysis of the spectrum in this frequencies range is complicated by the fact that when a complex is formed we have to account for the splitting of the F_2 levels together with the occurrence of the overtone levels, all occurring in a narrow frequency range with possible complications of Fermi resonances which generate intensity borrowing. This kind of situation, associated to a complexed $TiCl_4$ unit, must be expected for both the monomeric and the dimeric octahedral species we are considering in this work.

3.2. FT-Raman spectra of chemically prepared precursors

FT-Raman spectra have been recorded also for $MgCl_2/TiCl_4$ samples obtained via chemical process. One of the samples was based on the $TiCl_4$ treatment (at 70 °C in hexane) of a solid $MgCl_2$ obtained in an activated (high surface area) form via HCl treatment of a dialkyl magnesium compound. In Fig. 4a, the

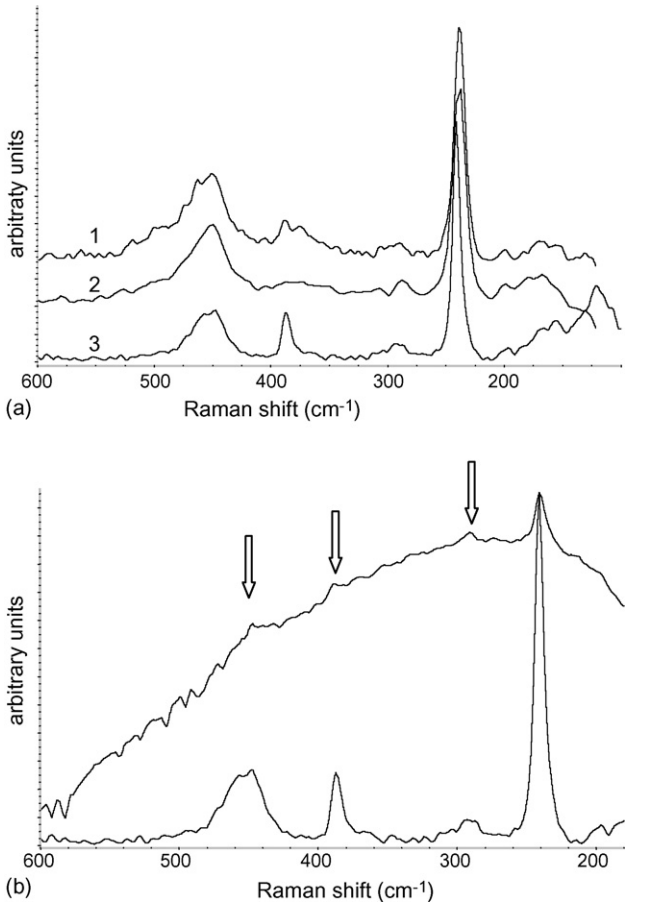

Fig. 4. (a) FT-Raman spectra of sample prepared from alkyl magnesium. Unwashed sample (1), washed sample (2) and unwashed $C_{10/1}$ (3). (b) FT-Raman spectra of sample prepared from dealcolated $MgCl_2$ (upper spectrum) and unwashed $C_{10/1}$. Arrows indicate the lines attributable to complexed $TiCl_4$ species.

Raman spectra of unwashed and washed (in hexane) sample are compared with that of the $C_{10/1}$. In the FT-Raman spectra of these samples, the same spectroscopic features of the mechanically prepared samples are found: Raman lines at 450, 386, 290,170, 137 and 120 cm^{-1} are observed and after washing only the bands at 450, 290 and 170 cm^{-1} survive.

One sample prepared starting from an $MgCl_2$/EtOH complex (more similar to an industrial catalyst synthesis) has been also considered. It shows a less clear FT-Raman spectrum with a high fluorescence emission (see Fig. 4b), but the signals which can be ascribed to $TiCl_4$ species complexed on $MgCl_2$ with Raman lines at 450, 386 and 290 cm^{-1} are still observed.

3.3. Experimental spectroscopic evidence

To summarize, from the experimental Raman spectra we derive the following spectroscopic information:

(a) the complexes $TiCl_4$–$MgCl_2$ show characteristic Raman lines in the region 600–100 cm^{-1} clearly distinguishable from those of the $MgCl_2$ crystal;

(b) the Raman lines of the complexes originate from vibrations which are mostly localized on the $TiCl_4$ molecules;
(c) atleast three different types of complexes are detected namely the *stable complex* with lines at 450, 290 and 170 cm^{-1}, the unstable complex with a strong line near 450 cm^{-1} and the *free species* (physisorbed) with lines at 386 and 120 cm^{-1};
(d) the washing process removes some *unstable* (*less stable*) complexes and the *free species*;
(e) the lines assigned to the *stable complex* are always observed in the Raman spectra of samples from different preparation techniques namely mechanical, chemical and industrial.

4. Discussion

4.1. Calculated Raman spectra

To rationalize the experimental results presented above, quantum chemical calculations have been carried out on a few molecular models. In our previous work [14] the study of a sample similar in preparation and Ti content to $C_{50/1}$ was presented. In that case a satisfactory agreement between the theoretical and experimental Raman data was obtained assuming a model of the complex along the (1 1 0) $MgCl_2$ lateral cut with the Ti atom in an octahedral coordination.

A concept so far not sufficiently stressed was that the Raman spectral pattern of the complex (i.e. number, frequencies and intensities of scattering lines) could be mainly determined by the geometry of the $TiCl_4$ molecule in going from the tetrahedral (free molecule) to the "new" structure (in the complex) with the Ti atom in an octahedral coordination geometry.

Starting from our previous results, new calculations have been carried out on models similar to those proposed by Corradini et al. [19] and generally accepted as the most plausible structure of the catalytic sites [2].

In particular, the existence of $TiCl_4$ momeric and Ti_2Cl_6 dimeric species complexed along the (1 1 0) and (1 0 0) lateral cuts have been introduced to account for the different stereospecificity (ability to form isotactic polypropylene) of the catalytic site. Corradini and co-workers proposed that the epitactic placement of dimeric Ti_2Cl_6 species (derived from the reduction of Ti_2Cl_8 with aluminium alkyls) on the (1 0 0) lateral cut could lead to the formation of stereospecific active sites [2,19], while the aspecific sites could be generated from monomeric $TiCl_4$ molecules complexed on the (1 1 0) lateral cut. On the basis of this model and in absence of Lewis bases, the (1 0 0) lateral cuts should be mostly covered by Ti_2Cl_8 stereospecific site, whereas non-stereospecific sites should occur on the (1 1 0) lateral cuts [2]. The dimeric octahedral complex is so far the most accepted conceptual model for the isospecific catalytic sites in the Ziegler–Natta catalysts.

We have performed several DFT calculations with PC-GAMESS [20] and GAMESS [21] ab initio quantum chemistry programs on the free tetrahedral $TiCl_4$ molecule in order to chose the functional that assures the best fit between calculated and experimental data. Different functional, namely: B88, XPBE96, CPBE96, VWN5, PBEPW91, B3LYP and PBE1PW91 (as reported in GAMESS and PC-GAMESS manuals) with the 631 g bases set, have been tested. All the calculated Raman spectra show spectral patterns very similar and in agreement with our previous results [14]. The PBE1PW91 (Perdew–Burke–Ernzerhof 1996 + Hartree–Fock exchange, Perdew 1991 non-local + Perdew–Wang 1991 LDA correlation) functional with 631 g basis produce a very good fit between calculated and experimental Raman spectra of free $TiCl_4$; we have adopted this level of theory for the calculation on our molecular models. More accurate results can be obtained using higher basis set. A slightly better fit was obtained using the same functional with a McLean/Chandler triple split but this choice was not applicable for calculations on larger complex models. Since the values of the calculated vibrational frequencies and the absolute vibrational infrared and Raman intensities are obviously basis set dependent, we use as a reliable structural tool only the qualitative trend and the qualitative intensity ratios and no arbitrary scaling factor has been applied to the calculated frequencies.

In our theoretical models, necessarily, only a finite numbers of atoms have been used to describe the complexes. The effect of the increasing size of the $MgCl_2$ cluster on the spectroscopic properties of the complexes has been critically investigated. In spite of this over-simplification the results turn out to be consistent showing the existence of vibrations localized on the $TiCl_4$ and weakly influenced by those of the $MgCl_2$ cluster.

Raman spectra were calculated after a partially constrained geometry optimisation, i.e. the internal coordinates of the $MgCl_2$ cluster (Mg–Cl bond length = 2.49 Å; Cl–Mg–Cl bond angle = 90°) have been keep fixed in order to mimic the $MgCl_2$ crystal structure of the support while those of $TiCl_4$ were left free to change.

The models studied in this work were:

- *Model 1*. $TiCl_4$ molecule complexed along the (1 1 0) $MgCl_2$ lateral cut with the Ti atom in an octahedral coordination (Fig. 5a);
- *Model 2*. $TiCl_4$ molecule complexed along the (1 1 0) $MgCl_2$ lateral cut with the Ti atom in a tetrahedral coordination (Fig. 5b);
- *Model 3*. Dimeric $TiCl_4$ species (Ti_2Cl_8) on the (1 0 0) $MgCl_2$ lateral cut with the Ti atoms in a tetrahedral coordination (Fig. 5c).

The fact that in both models 1 and 3 the $TiCl_4$ molecules appear with the Ti atoms in an octahedral coordination cannot be neglected. This is discussed more in depth below.

In order to elucidate the influence of the size of the crystalline substrate, different clusters of $MgCl_2$ have been considered for case 1. In Fig. 6a, the calculated Raman spectra are reported (for clarity we show only the few lines that originate from vibrations mostly localized on the $TiCl_4$ molecule, as indicated by calculations). The Raman active modes localized on the $TiCl_4$ molecule show the same spectral pattern with two main lines located near 460 and 300 cm^{-1} and the intensities increase as the dimensions of the $MgCl_2$ clusters increase.

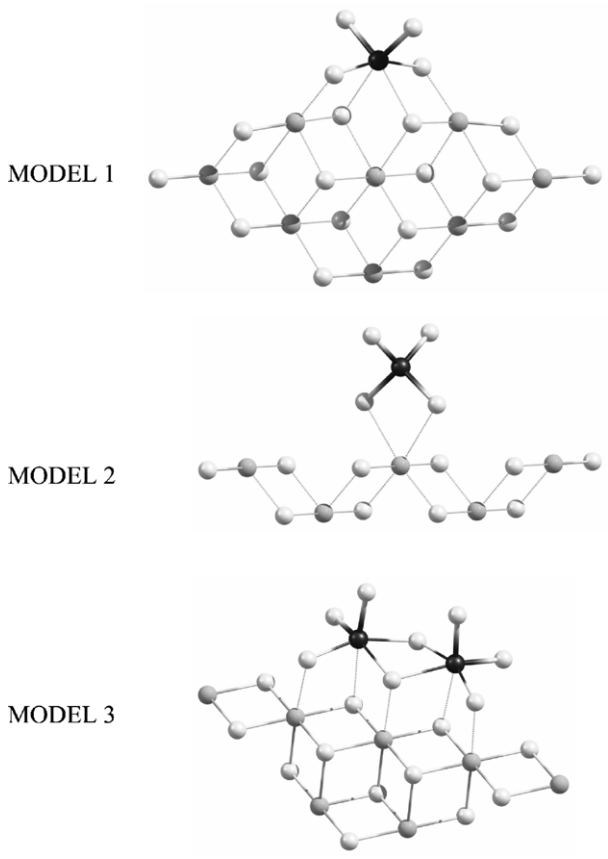

Fig. 5. Molecular models used to calculate the Raman spectra: model 1, $TiCl_4$ molecule complexed along the 1 1 0 $MgCl_2$ lateral cut in an octahedral coordination; model 2, $TiCl_4$ molecule complexed along the 1 1 0 $MgCl_2$ lateral cut in a tetrahedral coordination; model 3, dimeric $TiCl_4$ species (Ti_2Cl_8) on the 1 0 0 $MgCl_2$ lateral cut. Colours: Ti (●), Mg (●) and Cl (●).

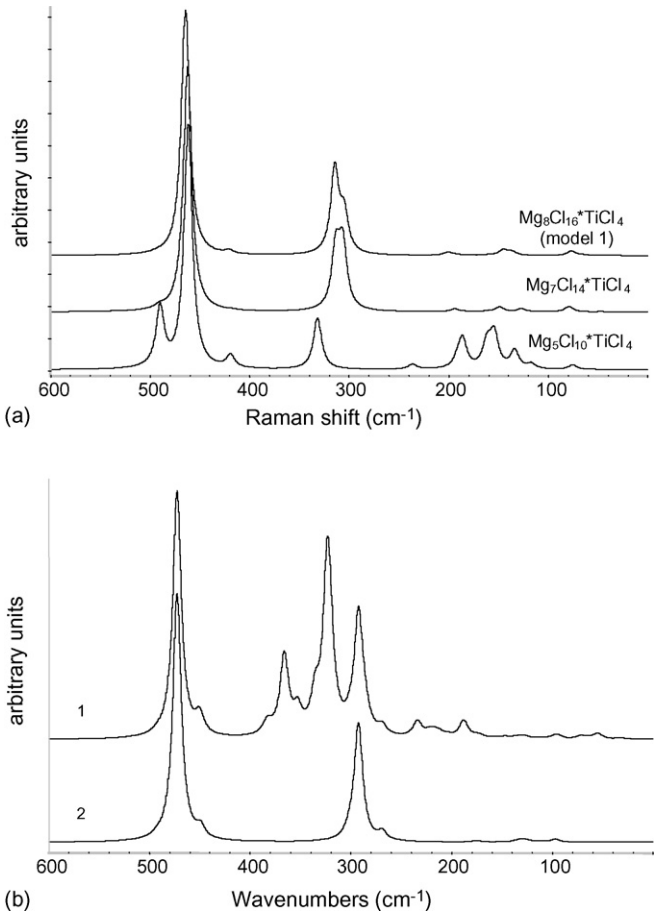

Fig. 6. (a) Calculated Raman spectra of $TiCl_4$ molecule complexed along the 1 1 0 $MgCl_2$ lateral cut in an octahedral coordination with increasing $MgCl_2$ cluster dimensions. Only the lines mostly localized on the $TiCl_4$ molecule, as indicated by calculations, are drawn. (b) Calculated Raman spectra of model 1 with the position of the four Mg and Cl atoms directly facing to $TiCl_4$ optimized (1). In (2) only the lines mostly localized on the $TiCl_4$ molecule, as indicated by calculations, are drawn.

The effect of the local rearrangement of the geometry of the $MgCl_2$ cluster has also been considered for model 1. For this purpose the four Mg and Cl atoms facing $TiCl_4$ have been allowed to change their position during the geometry minimization process and the calculated Raman spectrum is displayed in Fig. 6b. Also in this case we found two lines near 460 and 300 cm^{-1} that can be ascribed to vibrations localized on $TiCl_4$. The many other lines calculated and shown in the spectrum of Fig. 6b are due to the finite dimensions of the $MgCl_2$ cluster considered and turn out to be Raman active because the size of the crystal is relatively small. As matter of fact in the real $MgCl_2$ crystal, because of translational symmetry, only the two $k = 0$ phonons at 240 and 152 cm^{-1} involving the cooperative motions of all Mg and Cl atoms can be Raman active.

It is apparent from these spectra that the dimensions as well as the geometrical parameters of the $MgCl_2$ cluster basically do not affect the vibrational properties of the complexed $TiCl_4$ molecule.

In Fig. 7, the calculated spectra of the three models of the complexes (only the lines originating from the $TiCl_4$ vibrations are displayed) and the experimental spectra of $C_{10/1}$ are reported.

For model 1 the fit between calculated (lines at 464 and 315 cm^{-1}) and experimental Raman spectrum of the *stable complex* is quite satisfactory.

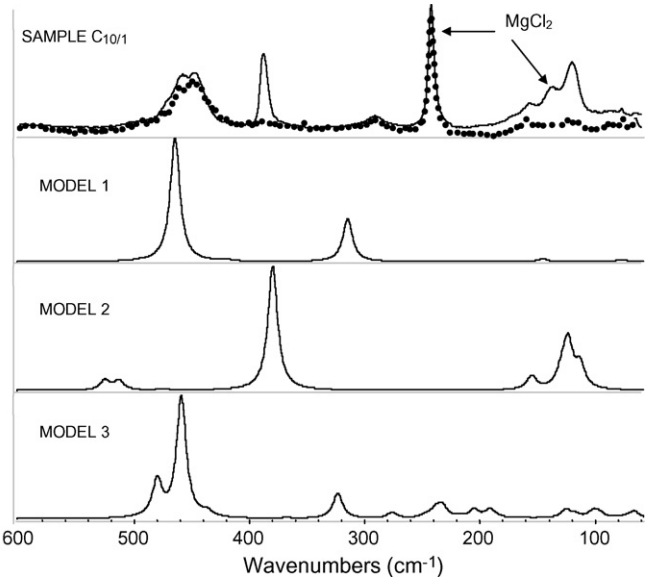

Fig. 7. Comparison between experimental Raman spectra of $C_{10/1}$ (washed sample dotted line and unwashed sample solid line) and calculated Raman spectra of models 1, 2 and 3.

The calculated Raman spectrum of model 2 fits very well with the lines at 386 and 120 cm^{-1}, already ascribed to free or physisorbed $TiCl_4$: model 2 certainly is not the stable complex.

Model 3 shows a strong Raman activity only in the region near 459 cm^{-1}: other weak lines are spread over a wide range of wavenumbers (322, 276, 234, 204, 191, 124 and 100 cm^{-1}).

An interesting issue arises by the fact that the calculated spectra for models 1 and 3 turn out to show some similarity mainly with the strongest Raman line near 450 cm^{-1}; as already stated above this is obvious because in both models the Ti atoms are in an octahedral coordination. On the other hand, this could be a preliminary very important conclusion namely the Raman lines occurring in the spectra of $TiCl_4/MgCl_2$ complexes can be explained only by taking into account species where Ti has an octahedral geometry.

However, the spectral pattern of model 1 with only two strong lines at 464 and 315 cm^{-1} (intensity ratio 464/315 = 3) is favoured with respect to that of model 3 where, besides the lines at 459 and 322 cm^{-1}, many other lines of comparable intensity are observed and the line at 322 cm^{-1} is weaker with respect to that of the model 1 (intensity ratio 459/322 = 8). Moreover, if the spectrum of model 1 with the position of Cl and Mg atoms directly complexed with the $TiCl_4$ have been minimized (see Fig. 6b), the fit turns out to be more acceptable.

In the literature many theoretical studies [22–25] and experimental works with different techniques namely extended X-ray absorption fine structure (EXAFS) [26,27], XPS [12,28], small and wide angle X-ray scattering (SAXS WAXS) [28–30], electron spin resonance (ESR) [31–33] and low energy electron diffraction (LEED) [34] have been devoted to investigate the nature of the catalytic site, often with divergent results. Recently energy calculations on molecular models similar to those studied in this work [22], indicate that the formation and the stability of $TiCl_4$ monomeric species complexed onto $MgCl_2$ are much more favoured with respect to the dimeric species. This conclusion turns out to be in accordance with our theoretical results on the Raman spectra.

4.2. Integrated intensity ratios of Raman lines of co-milled precursors

Additional information on the nature of the $TiCl_4$–$MgCl_2$ complexes are obtained form the study of the integrated intensities of the Raman lines of the stable and unstable complexes. We focus our attention on three Raman lines:

(1) the 240 cm^{-1} of the bulky $MgCl_2$, chosen as internal reference;
(2) the 450 cm^{-1} of the complexed $TiCl_4$ with contributions from the stable and unstable complexes;
(3) the 290 cm^{-1} assigned to the stable complexes only.

The experimental Raman line intensity ratios I_{450}/I_{240} and I_{290}/I_{240} at different Ti/Mg concentrations for the washed and unwashed samples are plotted in Fig. 8.

In Fig. 8, a linear relationship of the intensity ratios versus the Ti content chemically determined from elemental analysis

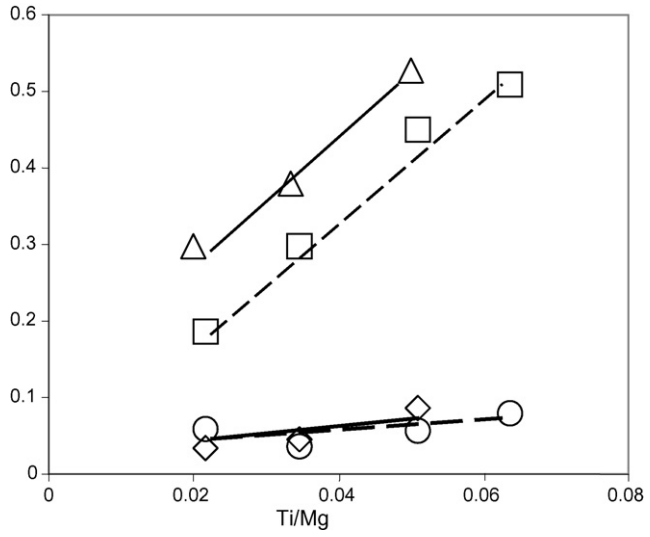

Fig. 8. Experimental values of integrated Raman intensity lines ratios: I_{450}/I_{240} (□) and I_{290}/I_{240} (◯) for washed and I_{450}/I_{240} (△) and I_{290}/I_{240} (◇) for unwashed samples at different Ti/Mg values (solid and dotted line are only guides to eyes).

can be clearly seen and from a least squares fitting of the data we obtain the following equations:

$$\frac{I_{450}}{I_{240}} = 7.93\left(\frac{\text{Ti}}{\text{Mg}}\right) + 0.02 \quad (1)$$

$$\frac{I_{450}}{I_{240}} = 1.42\left(\frac{\text{Ti}}{\text{Mg}}\right) - 0.01 \quad (2)$$

for the washed samples and

$$\frac{I_{450}}{I_{240}} = 7.68\left(\frac{\text{Ti}}{\text{Mg}}\right) + 0.14 \quad (3)$$

$$\frac{I_{450}}{I_{240}} = 1.74\left(\frac{\text{Ti}}{\text{Mg}}\right) - 0.01 \quad (4)$$

for the unwashed samples.

In the first case (Eqs. (1) and (2)) only the stable complexes can contribute to the intensity of the Raman lines; the linear dependency in a wide range of Ti content can be related to the linear increase of the number of sites where complexation takes place when the mean dimensions of the crystallites decrease (see Table 1) and nicely shows that the lines at 450 and 290 cm^{-1} originate only from a single chemical species (stable complexes).

In the second case both stable and unstable complexes can contribute to the intensities of lines near 450 cm^{-1}. Whereas the values of I_{290}/I_{240} ratios are practically similar to the first case (confirming that the lines at 290 cm^{-1} originate only from the stable complexes) the values of I_{450}/I_{240} are systematically higher (approximately 0.14) Fig. 8. The removed species, necessarily, must have been complexed at sites different from those of the stable species; moreover, the relative number of these sites does not increase with the activation process.

It can be concluded that the contribution to the intensity of the lines at 450 cm^{-1} due to the removed species is practically constant for every sample, thus indicating that the relative number

of these complexes is independent both from the Ti content and the dimensions of the $MgCl_2$ crystallites.

From the experimental X-ray data [35] it is reported that lateral cuts corresponding to the planes (1 1 0) and (1 0 0) are formed during the milling process. Theoretical energy calculations of the electrostatic energies on the $MgCl_2$ crystal indicates that the formation of (1 1 0) lateral cuts is favoured with respect to (1 0 0) lateral cuts [2]. Recently, a high resolution transmission electron microscopy (HRTEM) study on ball milled $MgCl_2$ [36] provides some evidence that most of the exposed coordinatively unsaturated Mg atoms lie along the (1 1 0) lateral cuts. Such considerations suggest that the number of (1 1 0) sites has to increase with the milling time or activation grade of the $MgCl_2$ more rapidly than the number of (1 0 0) sites, and can account for the two observed trends in the Raman intensities ratios. The stable complexes, whose number increases with increasing $TiCl_4$ content, are formed along the (1 1 0) lateral cut while the unstable complexes, whose number remains approximately constant with increasing $TiCl_4$ content, are complexed along the (1 0 0) lateral cut. Necessarily, along the (1 0 0) lateral cut the molecules of $TiCl_4$ have to complexed as dimers [19].

The linear dependency of the I_{450}/I_{240} ratio with the measured Ti/Mg ratio for the washed samples (Eq. (1)) could be proposed as master curve to determine, with a simple FT-Raman experiment, the $TiCl_4$ content in a sample.

Indeed we can express the recorded intensity for the lines at $450\,cm^{-1}$ as:

$$I_{450} = N_{TiCl_4}\alpha_{450} \tag{5}$$

where N_{TiCl_4} is the molar ratio of $TiCl_4$ units and α_{450} is the Raman scattering coefficient of a single unit. Similarly for the $MgCl_2$ line at $240\,cm^{-1}$ we can express the intensity as:

$$I_{240} = M_{MgCl_2}\alpha_{240} \tag{6}$$

thus the ratio turns out to be:

$$\frac{I_{450}}{I_{240}} = \left(\frac{\alpha_{450}}{\alpha_{240}}\right)\left(\frac{N_{TiCl_4}}{M_{MgCl_2}}\right) \tag{7}$$

It is thus possible to obtain the percentage content of $TiCl_4$ in a generic sample using the relation:

$$TiCl_4\,(\%) = \left(\frac{I_{450}}{I_{240}}\right)\left(\frac{\alpha_{240}}{\alpha_{450}}\right) \times 100 = \left(\frac{I_{450}}{I_{240}}\right)\frac{1}{7.93} \times 100 \tag{8}$$

where the value $\alpha_{450}/\alpha_{240} = 7.93$ is taken from the linear fit of the experimental data (Eq. (1)) and the I_{450}/I_{240} value has to be experimentally measured.

5. Conclusion

Starting with the analysis of the experimental FT-Raman spectra evidences are found that during the precatalyst preparation the $TiCl_4$ molecules "react" with $MgCl_2$ forming three different types of complexes. Two of these (the unstable ones) are easily removed by washing with solvent while the remaining (the stable one), is the only one that can be found in the washed samples.

The Raman signals characteristic of these complexes are:

(i) lines at 450 and $290\,cm^{-1}$ (stable complex);
(ii) lines at $450\,cm^{-1}$ removed by washing with *n*-hexane (unstable complex);
(iii) lines at 386, 137 and $120\,cm^{-1}$ (free or chemisorbed $TiCl_4$ molecules).

From the values of the intensity ratios of the lines at 450 and $290\,cm^{-1}$ with respect to the $242\,cm^{-1}$ of $MgCl_2$ chosen as internal reference, it is possible to derive a further clear indication of the occurrence of different complexed species that contribute to the intensity of the $450\,cm^{-1}$; the stable complexes contribute linearly with the increasing content of titanium, while the unstable complexes seem to contribute with a relative constant value. It is a noteworthy fact that Eq. (1) (unwashed samples) and Eq. (3) (washed samples) differ only for the intercept, suggesting that (i) the number of the stable complexes is not lowered by the washing process and (ii) stable and unstable complexes have, to lie on different crystal sites.

DFT quantum chemical calculations have been carried out on molecular models to predict the Raman spectra. The calculated Raman spectra of models 1 and 3 are similar and can explain the experimental Raman lines, but some important differences can be observed: namely model 3 shows a strong line only near $460\,cm^{-1}$ (many other weak lines are spread in a wide region), whereas model 1 in addition to the intense $460\,cm^{-1}$ shows a line with appreciable intensity at $290\,cm^{-1}$; the simultaneous occurrence of these two lines in the experimental spectrum can be interpreted as the *finger print* of the stable complex.

As a matter of fact, in the experimental spectra of both unwashed and washed samples the line near $290\,cm^{-1}$ is clearly detected and its intensity remains unchanged after the solvent washing. This observation is in line with a probable more stable $TiCl_4$ complex on 1 1 0 lateral cuts of $MgCl_2$ crystallites (model 1). The less stable and minority species could be the dimeric Ti_2Cl_8 complexes on the (1 0 0) cuts (model 2).

Quantum chemical energy calculations [22] support these hypotheses because the monomeric species along (1 1 0) lateral cuts were found to have an higher complexation energy on $MgCl_2$ crystal with respect to the dimeric species on the (1 0 0) lateral cuts.

The experimental observations can then be summarized as follows:

- during the milling process monomeric and dimeric species are formed;
- the monomeric species easily complex along the (1 1 0) lateral cuts;
- the dimeric species hardly complex along the (1 0 0) lateral cuts;
- as a consequence the number of complexes along the (1 1 0) increases with the Ti content while the number of complexes along the (1 0 0) lateral cut remains nearly constant;
- the dimeric species are removed by washing with solvents;

- the monomeric species that are stable originate the characteristic Raman spectrum with the "finger print" lines at 450 and 290 cm^{-1};
- the same spectral pattern is also found in samples prepared by chemical reactions;
- the monomeric species are therefore the prototype of the complex of $TiCl_4$ with the $MgCl_2$ also in the true catalytic systems.

The suggested model for the active sites in $MgCl_2/TiCl_4$ catalyst precursors heavily relies on the reading of the Raman spectrum which, however, turns out to be straightforward since it consists of a few lines whose origin is confidently and reasonably assigned by DFT calculations.

Acknowledgments

We thank Carlo Pelliciari for the recording of the FT-Raman spectra and Antonio Cristofori for the preparation of solid catalyst precursors.

References

[1] E. Albizzati, U. Giannini, G. Collina, L. Noristi, L. Resconi, in: E.P. Moore Jr. (Ed.), Polypropylene Handbook, Carl Hanser Verlag, Munich, 1996, p. 11.
[2] U. Giannini, G. Giunchi, E. Albizzati, P.C. Barbè, in: M. Fontanille, A. Guyot (Eds.), Recent Advances in Mechanistic and Synthetic Aspects of Polymerization, NATO ASI Sect. 215, Reidel, 1987, p. 473.
[3] P. Corradini, V. Busico, G. Guerra, in: G.C. Eastmann, A. Ledwith, S. Russo, P. Sigwalt (Eds.), Comprehensive Polymer Science, vol. 4, Pergamon Press, Oxford, 1989, p. 29.
[4] L. Barino, R. Scordamaglia, Macromol. Chem. Theor. Simul. 7 (1998) 407.
[5] E. Ritter, Ø. Nirisen, S. Kvisle, M. Ystenes, H.A. Øye, in: R.P. Quirk (Ed.), Transition Metal Catalyzed Polymerizations, Cambridge University Press, Cambridge, 1988, p. 292.
[6] M. Terano, T. Kataoka, T. Keii, J. Polym. Sci. Part A: Polym. Chem. 28 (1990) 2035.
[7] R. Spitz, J.L. Lacombe, A. Guyot, J. Polym. Sci. Part A: Polym. Chem. 22 (1984) 264.
[8] J.C.W. Chien, J.C. Wu, C.I. Kuo, J. Polym. Sci. Part A: Polym. Chem. 21 (1983) 725.
[9] Ø. Bache, M. Ystenes, Appl. Spectrosc. 48 (1994) 985.
[10] V. Di Noto, D. Fregonese, A. Marigo, S. Bresadola, Macromol. Chem. Phys. 199 (1998) 633.
[11] Ø. Bache, M. Ystenes, Proceedings of the International Symposium on Metallorganic Catalysts for Synthesis and Polymerization, Hamburg, September 13, 1998.
[12] E. Magni, G.A. Somorjai, J. Phys. Chem. B 102 (1998) 8788.
[13] M.J. Pilling, A. Amierio Fonseca, M.J. Cousin, K.C. Waugh, M. Surman, P. Gardner, Surf. Sci. 587 (2005) 78.
[14] L. Brambilla, G. Zerbi, S. Nascetti, F. Piemontesi, G. Morini, Macromol. Symp. 213 (2004) 287.
[15] R.J. Capwell, Chem. Phys. Lett. 12 (3) (1972) 443.
[16] H. Sano, H. Miyaoka, T. Kuze, H. Mori, G. Mizutani, N. Otsuka, M. Terano, Surf. Sci. 502/503 (2002) 70.
[17] R.J. Clark, B.K. Hunter, J. Chem. Soc. A 19 (1971) 2999.
[18] E.B. Wilson, J.C. Decius, P.C. Cross, Molecular Vibration. The Theory of Infrared and Raman Vibrational Spectra, McGraw-Hill Book Company, New York, 1955.
[19] P. Corradini, U. Barone, R. Fusco, G. Guerra, Gazz. Chim. Ital. 113 (1983) 601.
[20] A.A. Granovsky, http://www.classic.chem.msu.su/gran/gamess/index.html.
[21] M.W. Schmidt, K.K. Baldridge, J.A. Boatz, S.T. Elbert, M.S. Gordon, J.H. Jensen, S. Koseki, N. Matsunaga, K.A. Nguyen, S.J. Su, T.L. Windus, M. Dupuis, J.A. Montgomery, J. Comput. Chem. 14 (1993) 1347.
[22] G. Monaco, M. Toto, G. Guerra, P. Corradini, L. Cavallo, Macromolecules 33 (2000) 8953.
[23] M. Seth, P.M.M. Margl, T. Ziegler, Macromolecules 35 (20) (2002) 7815.
[24] C. Martinnsky, C. Minot, J.M. Ricart, Surf. Sci. 490 (2001) 237.
[25] E. Puhakka, T.T. Pakkanen, T.A. Pakkanen, Surf. Sci. 334 (1995) 289.
[26] A.G. Potapov, V.V. Kriventsov, D.I. Kochubey, G.D. Bukatov, V.A. Zakharov, Macromol. Chem. Phys. 198 (1997) 3477.
[27] P.J.V. Jones, R.J. Oldman, in: W. Kaminsky, H. Sinn (Eds.), Transition Metals and Organometallics as Catalysts for Olefin Polymerization, Springer, Berlin, 1988, p. 223.
[28] S.H. Kim, G.A. Somorjai, J. Polym. Chem. 104 (2000) 5519.
[29] H. Mori, K. Hasebe, M. Terano, J. Mol. Catal. A: Chem. 140 (1999) 16.
[30] A. Marigo, C. Marega, R. Zanetti, G. Morini, G. Ferrara, Eur. Polym. J. 36 (9) (2000) 1921.
[31] J.C.W. Chien, J.C. Wu, J. Polym. Sci. 20 (1982) 2445.
[32] J.C.W. Chien, J.C. Wu, J. Polym. Sci. 20 (1982) 2461.
[33] J.C.W. Chien, P.L. Bres, J. Polym. Sci. Part A 24 (1986) 2483.
[34] J.G. Roberts, M. Gierer, D.H. Fairbrother, M.A. Van-Hove, G.A. Somorjai, Surf. Sci. 399 (1998) 123.
[35] U. Giannini, Makromol. Chem. Suppl. 5 (1981) 216.
[36] H. Mori, M. Sawada, T. Higuchi, K. Hasebe, N. Otsuka, M. Terano, Macromol. Rapid Commun. 20 (1999) 245.